

CHROM. 9672

APPLICATION OF HIGH-PRESSURE GAS CHROMATOGRAPHY WITH COLUMNS PACKED WITH SMALL PARTICLES

H. H. LAUER, H. POPPE and J. F. K. HUBER*

Laboratory for Analytical Chemistry, University of Amsterdam, Nieuwe Achtergracht 166, Amsterdam (The Netherlands)

(Received June 29th, 1976)

SUMMARY

The application of high-pressure gas chromatography using columns with an I.D. of 1.0 mm, packed with small porous particles (below 60 μm), coated with a non-polar or polar stationary liquid, is described.

Plots of the theoretical plate height as a function of the mobile phase velocity demonstrate the low mixing characteristics of this type of column. A linear relationship was found between the number of theoretical plates and column length at a high ratio of the inlet and outlet pressures; 55,000 theoretical plates could be achieved at an inlet pressure of 44 bar with a 6-m long column.

For use in solving separation problems by gas chromatography, a nomogram has been derived that enables the proper conditions to be chosen. Some chromatograms that demonstrate the potential of these columns are presented.

Finally, an example of the dependence of the retention behaviour on the average column pressure is shown.

INTRODUCTION

In order to achieve large numbers of theoretical plates with packed columns in gas chromatography (GC), several investigators¹⁻³ used long columns while others^{4,5} also used columns of small diameter. In previous work⁶, we introduced GC columns packed with particles of small diameter, which consequently required a high inlet pressure. The ratio of particle diameter (d_p) to column diameter (d_c) with these columns was small (d_p/d_c down to 0.03) and it was shown that such columns have an extremely small theoretical plate height.

In this paper, the application of such types of columns with large numbers of theoretical plates (up to 50,000) is demonstrated.

* Present address: Institute of Analytical Chemistry, University of Vienna, Währinger Strasse 38, Vienna, Austria.

THEORETICAL

The implications of an increase in the column length and consequently in the pressure drop on the average theoretical plate height in GC were studied about 20 years ago¹⁻³. From the results of investigations of the influence of the particle size on the theoretical plate height in liquid chromatography⁷⁻¹⁰, it was concluded theoretically and verified experimentally⁶ that a significant decrease in the theoretical plate height by reducing the particle size can also be obtained in GC. In such columns a high pressure drop occurs and, if the column outlet pressure (p_L) is low (e.g., atmospheric), a high pressure ratio results.

If the GC apparatus has a given pressure limit and a given number of theoretical plates (N_R) is required in order to achieve the desired resolution, then the questions arise of the particle size and the column length that are necessary to obtain the required number of theoretical plates in the shortest possible separation time.

Knox and Saleem¹¹ solved this problem by using an empirical approach. They concluded that the minimum separation time is obtained when the particle size is such that at the available pressure the column operates at the minimum of the theoretical plate height *versus* flow velocity graph. Their solution is valid only if the minimum value of the reduced plate height (plate height divided by particle size) is the same for all particle sizes. Their results can be summarized as follows. The maximum speed of separation is obtained when

$$d_p = C_1 N_R^{\frac{1}{2}} p_0^{-1} \quad (1)$$

$$L = C_2 N_R^{\frac{3}{2}} p_0^{-1} \quad (2)$$

$$t_{R0} = C_3 N_R^2 p_0^{-1} \quad (3)$$

where

d_p = mean particle diameter;

N_R = number of theoretical plates required to obtain a given resolution (R);

p_0 = column inlet pressure;

L = column length;

t_{R0} = retention time of an unretarded component.

C_1 - C_3 are proportionality factors, which depend on both geometrical factors and physical constants. The complete derivation yields

$$C_1 = (D_{im}^L)^{\frac{1}{2}} h_m^{\frac{1}{2}} P e_m^{\frac{1}{2}} \varphi^{-\frac{1}{2}} \eta^{\frac{1}{2}} p_L^{\frac{1}{2}} \cdot \frac{3}{2} \cdot \frac{\pi (\pi^2 + 1)^{\frac{1}{2}} (\pi^2 - 1)^{\frac{1}{2}}}{(\pi^3 - 1)} \quad (4)$$

$$C_2 = (D_{im}^L)^{\frac{1}{2}} h_m^{\frac{3}{2}} P e_m^{\frac{1}{2}} \varphi^{-\frac{1}{2}} \eta^{\frac{1}{2}} p_L^{\frac{1}{2}} \cdot \frac{27}{16} \cdot \frac{\pi (\pi^2 + 1)^{\frac{3}{2}} (\pi^2 - 1)^{\frac{3}{2}}}{(\pi^3 - 1)^3} \quad (5)$$

$$C_3 = h_m^2 \varphi^{-1} \eta^{\frac{1}{2}} \cdot \frac{27}{16} \cdot \frac{\pi (\pi^2 + 1)^2 (\pi^2 - 1)^2}{(\pi^3 - 1)^3} \quad (6)$$

where

D_{im}^L = diffusion coefficient of component i in the mobile phase at the column outlet pressure;

h_m = minimum value of the local reduced theoretical plate height;

$Pe_m = u_z d_p / D_{im}^L$ = Peclet number at the minimum value of the theoretical plate height;

φ = shape factor of permeability, defined as:

$$\varphi = \frac{u_z \eta}{\frac{dp}{dz} \cdot d_p^2} \left[= \frac{4}{3} \cdot \frac{\pi (\pi^3 - 1)}{(\pi^2 - 1)^2} \cdot \frac{\bar{u} L \eta}{d_p^2 p_0} \right];$$

η = viscosity of the carrier gas;

p_L = column outlet pressure;

$\pi = p_0 / p_L$ = ratio of inlet and outlet pressures.

The factors C_1 – C_3 can be treated as constant because: (a) the physical constants D_{im}^L , p_L and η are constant; (b) for columns with a certain type of packing material the values of h_m , Pe_m and φ are found to be the same, as can be expected on theoretical grounds and has been shown experimentally; (c) the factors containing π in eqns. 4–6 are virtually constant for $\pi \geq 3$, which is illustrated by Table I.

TABLE I
FACTORS OF EQNS. 4–6 CONTAINING π

π	Corresponding factor		
	Eqn. 4	Eqn. 5	Eqn. 6
1.5	1.909	1.934	3.118
2.0	1.660	1.715	2.214
3.0	1.548	1.649	1.840
5.0	1.511	1.656	1.723
10.0	1.501	1.675	1.692
∞	1.500	1.688	1.688

Eqns. 4–6 differ from those obtained by Knox and Saleem¹¹ by the factor $\frac{9}{8} \cdot [(\pi^2 + 1)(\pi^2 - 1)^2] / [(\pi^3 - 1)^2]$, which is included in their treatment in h , by defining $h = \hat{H} / d_p$, where \hat{H} is the observed average value of theoretical plate height. It is more correct, however, to define h as H_z / d_p , where H_z is the local theoretical plate height at position z in the column. The difference is numerically negligible in practice.

EXPERIMENTAL

Apparatus

The high-pressure GC (HPGC) system used has been described earlier⁶. The sensitivity of the system was improved, however, by replacing the micro TCD with an FID (Tracor) and the manual sampling valve by a pneumatically driven sampling valve (Valco ACV-6-HTax) that could withstand higher temperatures (up to 300°).

The sample loop had a volume of $12 \mu\text{l}$. In combination with the internal valve volume, the total injection volume was about $20 \mu\text{l}$. The total dead volume outside the column of the system was less than $60 \mu\text{l}$.

The columns were prepared from stainless-steel tubing with an I.D. of 1.0 mm and a length of 1.50 m. Longer columns were prepared by coupling these standard columns to give the desired length by means of home-made stainless-steel low-volume fittings (dead volume less than $5 \mu\text{l}$).

Chemicals and materials

In the preparation of GC column packings, the following solid supports were used: Spherosil XOC-005 (Rhône-Poulenc, Paris, France) and Perisorb A (Merck, Darmstadt, G.F.R.). Appropriate particle size ranges were prepared by sieving (above $60 \mu\text{m}$) and wind-sifting (below $60 \mu\text{m}$). Squalane and PEG-6000 (GC grade, Merck) were used as stationary liquids.

The sample compounds used for the determination of the \bar{H} versus \bar{u} graphs were methane (high-purity grade, Matheson, Coleman & Bell, East Rutherford, N.J., U.S.A.), *n*-pentane and *n*-hexane (GC grade, Aldrich, Milwaukee, Wisc., U.S.A.), methyl ethyl ketone and diethyl ketone (GC grade, BDH, Poole, Great Britain).

The carrier gases were nitrogen (high-purity quality, L'Air Liquide, Paris, France) and helium (high-purity quality, Hoekloos, Amsterdam, The Netherlands).

Synthetic sample mixtures for separation experiments were prepared from compounds delivered by various manufacturers [Merck, Fluka (Buchs, Switzerland) BDH and Aldrich] and, if possible, GC grade materials were used.

RESULTS AND DISCUSSION

Our intention was to develop packed GC columns with high separation efficiencies for difficult separations, especially for trace analysis and direct coupling with a mass spectrometer. To show the potential of this type of column, a column of length 6 m was used.

Theoretical plate height

In Fig. 1, plots of the average theoretical plate height, \bar{H} , versus the average mobile phase velocity, \bar{u} , are shown for different carrier gases. A column length of 6 m and an average particle size of $55 \mu\text{m}$ were used. Both the sample and the stationary liquid were non-polar.

The plot for this 6-m column is closely similar to that of an analogous 1.5-m column measured earlier⁶. The larger pressure drop of the longer column does not change the observed minimum theoretical plate height significantly.

The shift of the minimum of the \bar{H} versus \bar{u} curve in helium to higher mobile phase velocities compared with nitrogen follows from the higher diffusion coefficient and the fact that the Peclet numbers for both columns are the same at the minimum of the \bar{H} versus \bar{u} curve (see Table II). One can also see that the slope of the rising branch of the curve is less in helium than in nitrogen, which is due mainly to the faster mass exchange of the sample in the mobile phase because of the larger diffusion coefficient in helium.

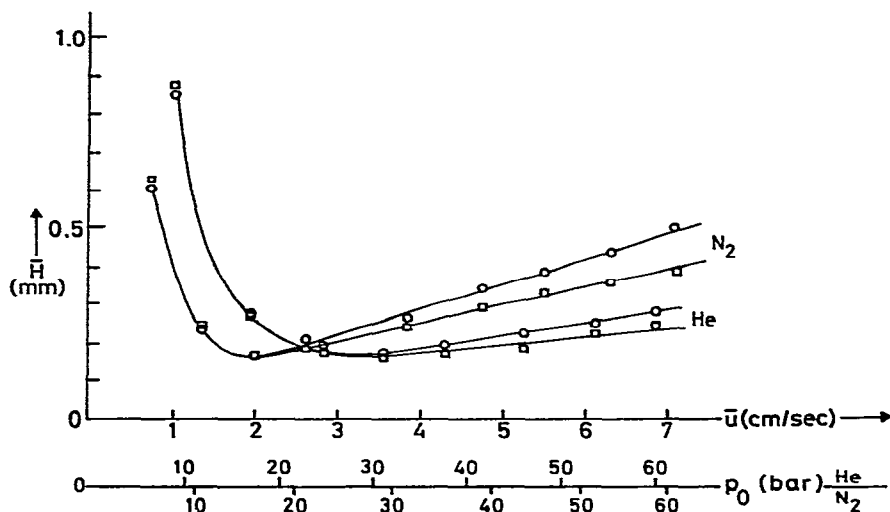


Fig. 1. \bar{H} versus \bar{u} curves for a packed column of length 6 m with 55- μm particles and different carrier gases. Column, 1.0 mm I.D., length 6 m; packing, Spherosil XOC-005, 50–60 μm , coated with 3.0% (w/w) silica; outlet pressure, atmospheric; carrier gases, nitrogen and helium; temperature, 80.0°; total dead volume outside the column, less than 60 μl . Sample: CH_4 , $\kappa \approx 0$; \square , *n*-pentane, $\kappa^{\text{He}} = 0.74$; \circ , *n*-hexane, $\kappa^{\text{He}} = 1.72$; sample pressure equal to column inlet pressure.

In Fig. 2, plots of \bar{H} versus \bar{u} are shown for a polar compound and a polar stationary liquid obtained with different carrier gases. The column length was 1.5 m and the average particle size 55 μm . The results and conclusions are very similar to those obtained with non-polar compounds and columns.

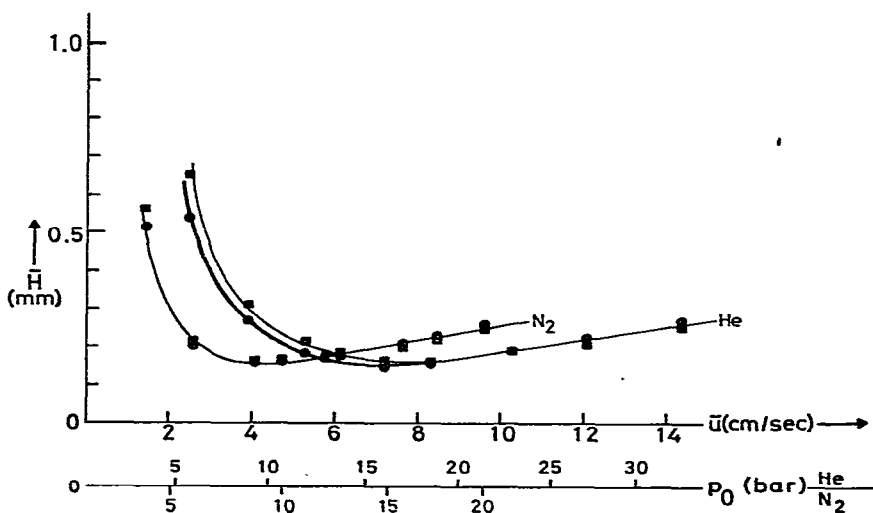


Fig. 2. \bar{H} versus \bar{u} curves for a packed column of length 1.5 m with 55- μm particles and different carrier gases. Column, 1.0 mm I.D., length 1.5 m; packing, Spherosil XOC-005, 50–60 μm , coated with 10.5% (w/w) PEG-6000; outlet pressure, atmospheric; carrier gases, nitrogen and helium; temperature, 80.0°. Sample: CH_4 , $\kappa \approx 0$; \blacksquare , methyl ethyl ketone, $\kappa^{\text{He}} = 4.66$; \bullet , diethyl ketone, $\kappa^{\text{He}} = 7.83$. Other conditions as in Fig. 1.

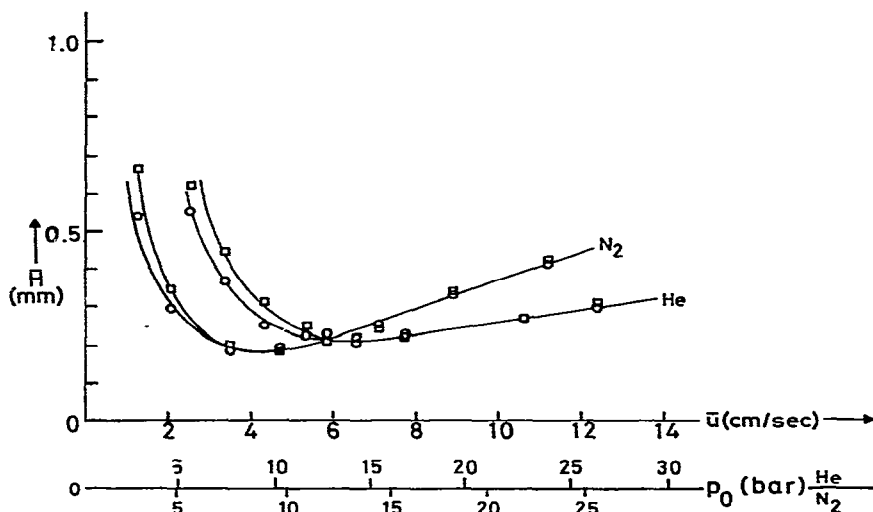


Fig. 3. \bar{H} versus \bar{u} curves for a packed column of length 1.5 m with 30–40- μm porous layer particles and different carrier gases. Column, 1.0 mm I.D., length 1.5 m; packing, Perisorb A, 30–40 μm , coated with 1.0% (w/w) squalane; outlet pressure, atmospheric; carrier gases, nitrogen and helium; temperature, 80.0°. Sample: CH_4 , $\kappa \approx 0$; \square , *n*-pentane, $\kappa^{\text{He}} = 2.16$; \circ , *n*-hexane, $\kappa^{\text{He}} = 5.29$. Other conditions as in Fig. 1.

In Fig. 3, \bar{H} versus \bar{u} plots in nitrogen and helium are shown for a support material that does not consist of completely porous particles but of porous layer beads. The column length was 1.5 m and the average particle size 30–40 μm . If we compare this column with another⁶ packed with totally porous particles of about the same size (30–35 μm) and coated with 3–4% (w/w) squalane, containing the same amount of stationary liquid in the column, considerable differences are found:

(1) The capacity factor (κ_t) of a solute measured on the porous layer bead column is about twice as high as that on the totally porous particle column. This effect is due to the fact that the phase ratio V_s/V_g , where V_s and V_g are the volumes of stationary liquid phase and the total gas phase in the column, respectively, for the porous layer bead column is twice as large as that for the totally porous particle column.

(2) The mobile phase velocity for which \bar{H} has a minimum is 1.6 times higher with the porous layer bead column. This observation can be explained by the fact that the gas volume in the totally porous particle column is about 1.6 times larger.

(3) The pressure drop over the porous layer bead column at the \bar{H} minimum is about three times smaller than that for the completely porous particle column. Two effects are responsible for this difference: the porous layer particles are more spherical and show a better adherence to the Kozeny–Carman relationship. The mobile phase velocity is equal to the interstitial velocity in the case of a porous layer bead packing.

In conclusion, one can say that the porous layer bead support material is very promising for this type of work.

Fig. 4 shows a plot of the number of theoretical plates versus the column length for different column packings. The linear plot indicates that the average theoretical

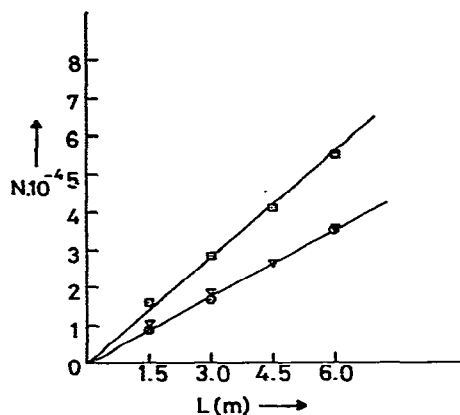


Fig. 4. Number of theoretical plates (N) versus column length (L) for coupled packed columns and different column packings. \circ , 50–60- μm particles. \square , 30–35- μm particles; sample, n -hexane; other conditions as in Fig. 1. ∇ , 50–60- μm particles; sample, diethyl ketone. Other conditions as in Fig. 2.

plate height is independent of column length and pressure, owing to the high pressure ratios involved. The agreement between the two columns with the same particle size but different sample components and stationary liquids is noteworthy.

Construction of a nomogram

With the aid of eqns. 1–3 it is possible to construct a nomogram (Fig. 5) that relates these equations graphically, assuming that the constants C_1 – C_3 are known.

These constants can be calculated from experimental data according to eqns. 4–6. Such data were determined for n -hexane on columns packed with Spherosil XOC-005 supporting 3–4% (w/w) squalane using helium and nitrogen as carrier

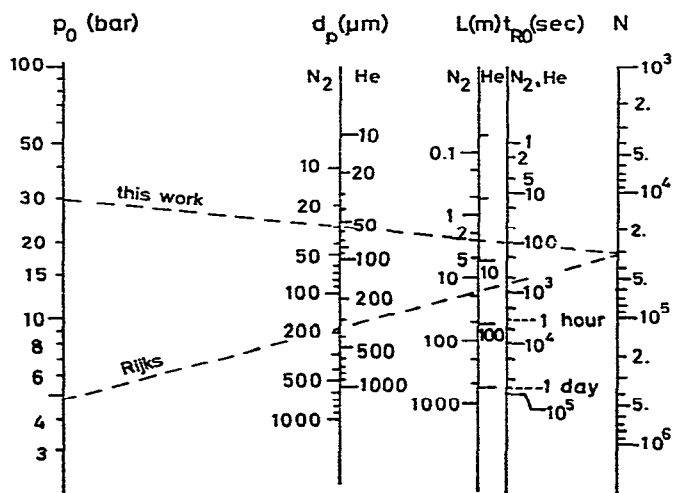


Fig. 5. Nomogram constructed with the aid of eqns. 1–6 and the characteristics of the various columns listed in Table II. The constants C_1 – C_3 are listed in Table III.

TABLE II

CHARACTERISTICS OF DIFFERENT NON-POLAR COLUMNS

Solute: *n*-hexane. Viscosity (80.0°; 1 bar) of nitrogen = $2 \cdot 10^{-4}$ g·cm⁻¹·sec⁻¹; viscosity (80.0°; 1 bar) of helium = $2.2 \cdot 10^{-3}$ g·cm⁻¹·sec⁻¹. Column outlet pressure (p_L) = 1 bar. Support material for all columns: Spherosil XOC-005 coated with 3-4% (w/w) squalane. Diffusivity (80.0°; 1 bar) of *n*-hexane in nitrogen = 0.11 cm²·sec⁻¹·bar; diffusivity (80.0°; 1 bar) of *n*-hexane in helium = 0.37 cm²·sec⁻¹·bar.

Parameter	Values									Average
φ	2.30	1.07	2.39	1.67	2.60	2.36	2.27	2.44		$\bar{\varphi} = 2.1$
h_m	2.53	3.76	2.86	3.00	3.09	3.18	3.05	3.31		$\bar{h}_m = 3.1$
Pe_m	1.54	1.18	1.03	1.15	1.02	1.08	1.08	1.32		$\bar{Pe}_m = 1.2$
d_p (μm)	200-250	120-140	63-71	30-35	50-60	50-60	50-60	50-60		—
L (m)	1.5	1.5	1.5	1.5	6.0	6.0	1.5	3.0		—
Carrier gas	N ₂	N ₂	N ₂	N ₂	N ₂	He	N ₂	N ₂		—

TABLE III

VALUES OF THE CONSTANTS IN EQNS. 1-3 FOR NON-POLAR COLUMNS

Constant	Carrier gas	
	N ₂	He
C_1 (bar·cm)	$9.2 \cdot 10^{-3}$	$1.8 \cdot 10^{-2}$
C_2 (bar·cm)	$3.2 \cdot 10^{-2}$	$6.2 \cdot 10^{-2}$
C_3 (bar·sec)	$1.5 \cdot 10^{-3}$	$1.7 \cdot 10^{-3}$

gases. They are listed in Table II and the calculated values of the constants C_1 – C_3 are given in Table III. They are constant to within 20% for all columns prepared from this support material for particle sizes between 250 and 30 μm.

From this nomogram the following conclusions can be drawn: (1) theoretical plate numbers in excess of 10^5 are possible in GC with packed columns and with reasonable retention times; (2) an increase in the pressure capability of the apparatus results in an inversely proportional increase in the speed of separation.

Two examples are shown on the nomogram (Fig. 5) for illustration. The upper dotted line results from this work. The corresponding column length was 6 m and the average particle size 55 μm, and the carrier gas was helium. The nomogram shows that one can expect about 30,000 theoretical plates for *n*-hexane with an inlet pressure of about 30 bar, which is very close to the measured value. The lower dotted line results from the work of Rijks¹².

As a result of the limited inlet pressure, in this instance about 5 bar with nitrogen, realization of a theoretical plate number of about 30,000 with a particle size of about 200 μm requires a column length of 15 m. As a consequence, a 6-fold increase in the separation time compared with the column with 55-μm particles is predicted. However, a factor of only 2 is observed experimentally (compare Fig. 9 in ref. 4 with Fig. 7 in this paper, with t_{R0} values of 313 and 159 sec, respectively). This result is due to the fact that the column prepared by Rijks shows excellent permeability and reduced plate height.

The nomogram was also checked for polar columns. The experimental data

TABLE IV

CHARACTERISTICS OF DIFFERENT POLAR COLUMNS

Solute: diethyl ketone. Viscosities and diffusivities (80.0°; 1 bar) as in Table II. Column outlet pressure (p_L) = 1 bar. Support material for all columns: Spherosil XOC-005 coated with 10.5% (w/w) PEG-6000.

Parameter	Values						Average
φ	2.37	2.26	2.07	2.23	2.17	2.27	$\bar{\varphi} = 2.2$
h_m	2.91	2.67	3.25	3.49	3.05	3.24	$\bar{h}_m = 3.1$
Pe_m	1.17	1.13	1.03	1.11	1.07	1.38	$\bar{Pe}_m = 1.2$
d_p (μm)	50-60	50-60	50-60	50-60	50-60	50-60	—
L (m)	1.5	1.5	1.5	1.5	1.5	6.0	—
Carrier gas	N ₂	He	He	He	He	He	—

TABLE V

VALUES OF THE CONSTANTS IN EQNS. 1-3 FOR POLAR COLUMNS

Constant	Carrier gas	
	N ₂	He
C_1 (bar·cm)	$8.9 \cdot 10^{-3}$	$1.7 \cdot 10^{-2}$
C_2 (bar·cm)	$3.1 \cdot 10^{-2}$	$6.0 \cdot 10^{-2}$
C_3 (bar·sec)	$1.5 \cdot 10^{-3}$	$1.6 \cdot 10^{-3}$

for these columns are listed in Table IV and the calculated values of the constants C_1 - C_3 are given in Table V.

From Tables III and V, it can be seen that the nomogram fits the data obtained from both non-polar and polar columns. In conclusion, it can be said that the nomogram, for this type of solid support material and perhaps for other types also, presents a universal and simple means for predicting the particle size and column length that should be used in order to solve a separation problem for which one needs a certain number of theoretical plates with a given pressure capability of the apparatus.

Separations

In order to show the ability of HPGC, a number of separations were carried out (Figs. 6-13). Figs. 6 and 7 demonstrate the separation speed that can be achieved in HPGC. The separation speed is defined as the maximum number of components that can be separated with a given resolution in a given time.

Defining the resolution of two components j and i as

$$R_{ji} = \frac{t_{Rj} - t_{Ri}}{\sigma_{ii}} \quad (t_{Rj} > t_{Ri}) \quad (7)$$

where

t_{Rj} and t_{Ri} = retention times of component j and i , respectively;
 σ_{ii} = standard deviation of the elution peak of component i ;

a virtually complete separation of two components present in about the same amounts is obtained if $R_{ji} = 6$. The speed of separation is not constant but decreases with time.

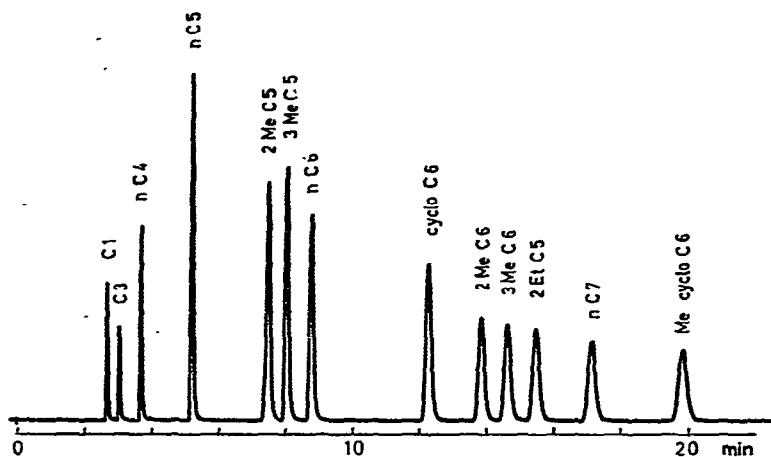


Fig. 6. Rapid separation of a hydrocarbon mixture. Column, 1.0 mm I.D., length 6 m; packing, Spherosil XOC-005, 50–60 μm , coated with 3.0% (w/w) squalane; outlet pressure, atmospheric; inlet pressure, 30 bar; carrier gas, helium; temperature, 70.0°; $N(\text{hexane}) = 33,000$, $\kappa = 2.23$; volume flow-rate at column outlet and ambient temperature (W_{aa}) = 22 ml·min⁻¹.

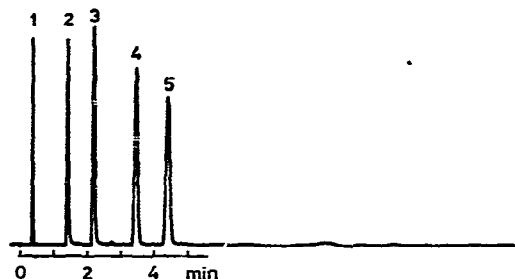


Fig. 7. Rapid separation of ketones. Column, 1.0 mm I.D., length 1.5 m; packing, Spherosil XOC-005, 50–60 μm , coated with 10.5% (w/w) PEG-6000; outlet pressure, atmospheric; inlet pressure, 15.9 bar; carrier gas, helium; temperature, 79.9°; $N(\text{cyclohexanone}) = 9900$, $\kappa = 51.4$; $W_{aa} = 21.4$ ml·min⁻¹. 1, methane; 2, acetone; 3, methyl ethyl ketone; 4, diethyl ketone; 5, isobutyl methyl ketone.

From Fig. 6, it can be seen that a speed of separation of about 20 components per 5 min, 40 components per 10 min and 60 components per 20 min was achieved with a theoretical plate number of 33,000. Fig. 7 indicates corresponding values of 40, 55 and 70 with a theoretical plate number of 10,000.

The increase in resolution that can be obtained with a 4-fold increase in column length is shown in Figs. 8 and 9.

It should be emphasized again that in HPGC the number of theoretical plates increases linearly with column length (see Fig. 4). At very high numbers of theoretical plates a small non-linearity of the distribution isotherm is sufficient to determine to a significant extent the peak width causing tailing of the peak. Under such circumstances, the increase in column length results in a distinct increase in peak tailing and little gain in resolution, as can be seen in Fig. 10.

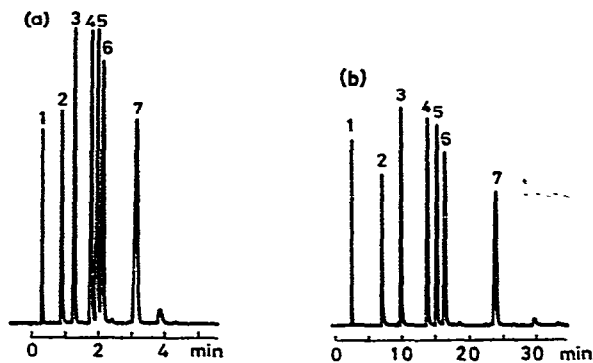


Fig. 8. Separation of esters on columns of different lengths. 1, Methane; 2, methyl formate; 3, methylacetate; 4, ethyl acetate; 5, methyl propionate; 6, *n*-propyl formate; 7, isopropyl propionate. Column length: (a) 1.5 m; (b) 6 m. *N*(ethyl butyrate): (a) 9000, $\kappa = 13.0$; (b) 33,500, $\kappa = 13.5$. Inlet pressure: (a) 15.9 bar; (b) 35.4 bar. Outlet flow-rate: (a) 21.4 ml·min⁻¹; (b) 26 ml·min⁻¹. Other conditions as in Fig. 7.

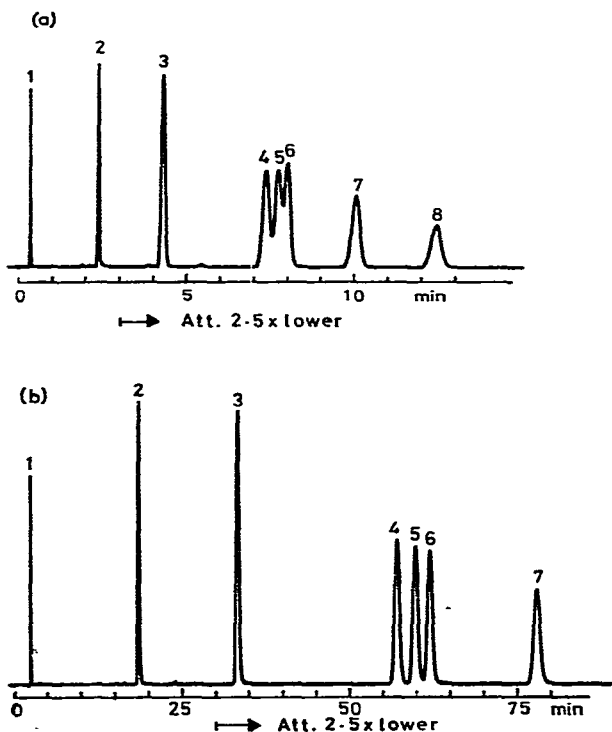


Fig. 9. Separation of light aromatic hydrocarbons on columns of different lengths. 1, Methane; 2, benzene; 3, toluene; 4, ethylbenzene; 5, *p*-xylene; 6, *m*-xylene; 7, *o*-xylene. Column length: (a) 1.5 m; (b) 6 m. *N*(*o*-xylene): (a) 8900, $\kappa = 27.6$; (b) 33,000, $\kappa = 30.2$. Inlet pressure: (a) 15.9 bar; (b) 35.4 bar. Outlet flow-rate: (a) 21.4 ml·min⁻¹; (b) 26 ml·min⁻¹. Other conditions as in Fig. 7.

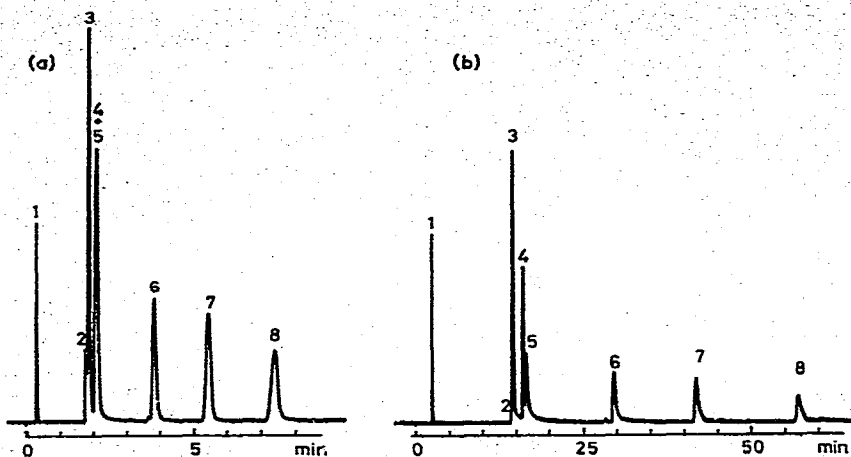


Fig. 10. Separation of lower alcohols on columns of different lengths. 1, Methane; 2, methanol; 3, *tert.*-butanol; 4+5, ethanol and 2-propanol; 6, 1-propanol; 7, isobutanol; 8, 1-butanol. Column length: (a) 1.5 m; (b) 6 m. $N(1\text{-butanol})$: (a) 7500, $\kappa = 20.4$; (b) 28,000, $\kappa = 22.0$. Inlet pressure: (a) 15.9 bar; (b) 35.4 bar. Outlet flow-rate (a) $21.4 \text{ ml}\cdot\text{min}^{-1}$; (b) $26 \text{ ml}\cdot\text{min}^{-1}$. Other conditions as in Fig. 7.

Examples of the practical application of HPGC are shown in Figs. 11–13. It can be seen that the separations of complex mixtures are comparable to those obtainable with capillary gas chromatography.

From Fig. 12, it can be concluded that a high number of theoretical plates (55,000 for *n*-hexane) can be achieved at such a small flow velocity that a low flow-rate

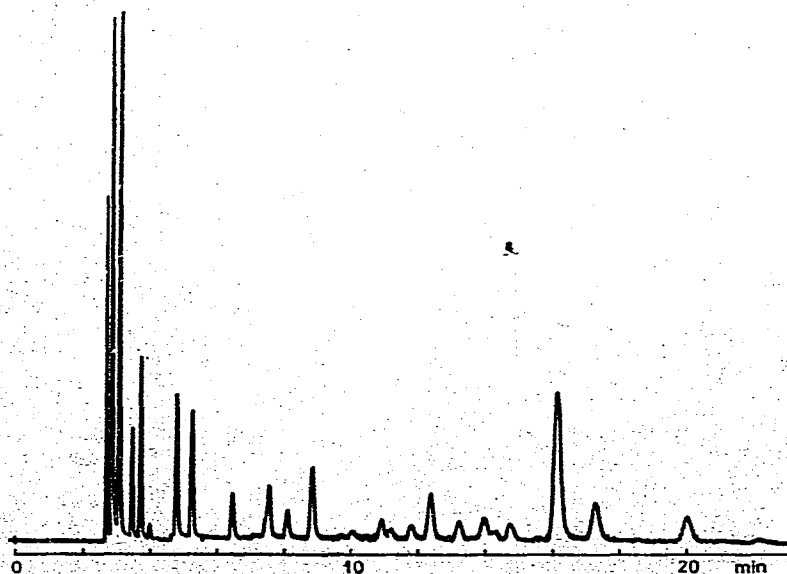


Fig. 11. Separation of Dutch natural gas. Conditions as in Fig. 6.

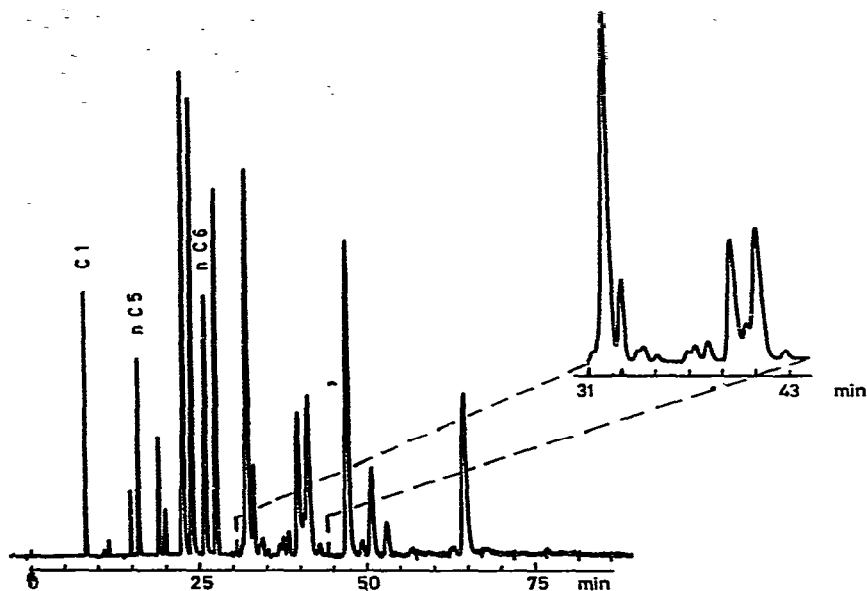


Fig. 12. Separation of petroleum spirit (b.p. 60–80°). Column dimension, outlet pressure and temperature as in Fig. 6; packing, Spherosil XOC-005, 30–35 μm , coated with 3.0% (w/w) squalane; inlet pressure, 44 bar; carrier gas, nitrogen; $N(n\text{-hexane}) = 55,000$, $\kappa = 2.12$; $W_{aa} = 12 \text{ ml}\cdot\text{min}^{-1}$.

at the column outlet ($12 \text{ ml}\cdot\text{min}^{-1}$) and a relatively large peak width (13.2 sec for *n*-hexane) are obtained.

These chromatographic characteristics allow the direct coupling of a packed column to a mass spectrometer without the need for a separator, and offer a sufficiently long scanning time for high-resolution mass spectra to be obtained.

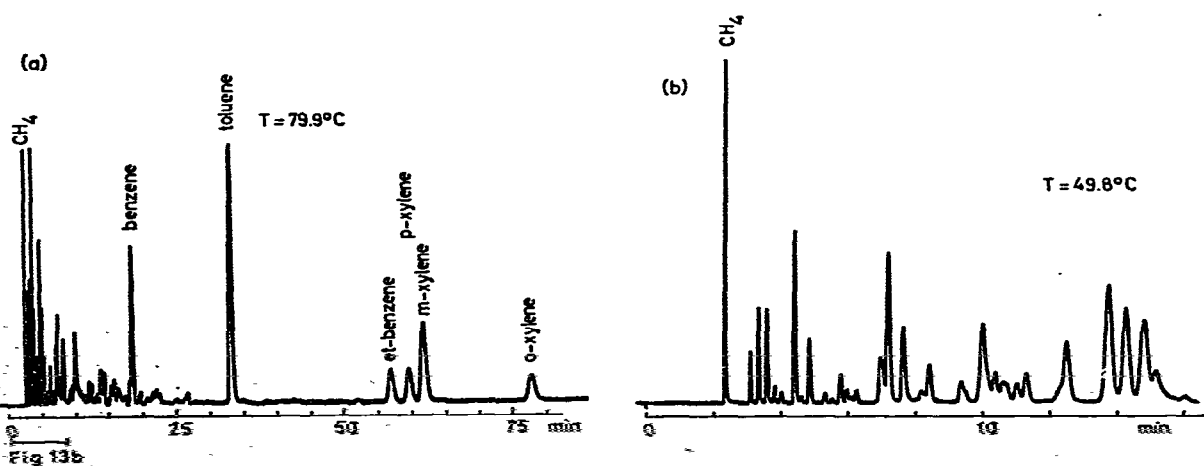


Fig. 13. Separation of regular gasoline (Shell) at different temperatures. Column, 1.0 mm I.D., length 6 m; packing, Spherosil XOC-005, 50–60 μm , coated with 10.5% (w/w) PEG-6000; outlet pressure, atmospheric; inlet pressure, 35.4 bar; carrier gas, helium. Temperature: (a) 79.9°; (b) 49.8°. Outlet flow-rate: (a) $26 \text{ ml}\cdot\text{min}^{-1}$; (b) shows a good resolution of the first part of (a).

Retention behaviour and average column pressure

In some separation experiments, it was noticed that the chromatograms of the same sample obtained with different carrier gases were different with respect to the relative positions of the peaks. This phenomenon can be explained^{13,14} as the result of significant interactions of the solutes with the carrier gases at high pressures.

In order to investigate this effect in more detail, the retention behaviour of several *n*-alkane homologues in nitrogen and helium was investigated. The results are shown in Fig. 14, where the logarithm of the capacity factor (κ) is plotted as function of the average column pressure (\bar{p}). The capacity factor and average column pressure are defined as:

$$\kappa_i = \frac{t_{Ri} - t_{R0}}{t_{R0}}$$

and

$$p = p_L/j$$

where

t_{Ri} = retention time of compound *i*;

t_{R0} = retention time of a non-retarded component;

P_L = column outlet pressure;

j = $\frac{3}{2} \cdot [(\pi^2 - 1)/(\pi^3 - 1)]$; compressibility factor with $\pi = p_0/p_L$;

p_0 = column inlet pressure.

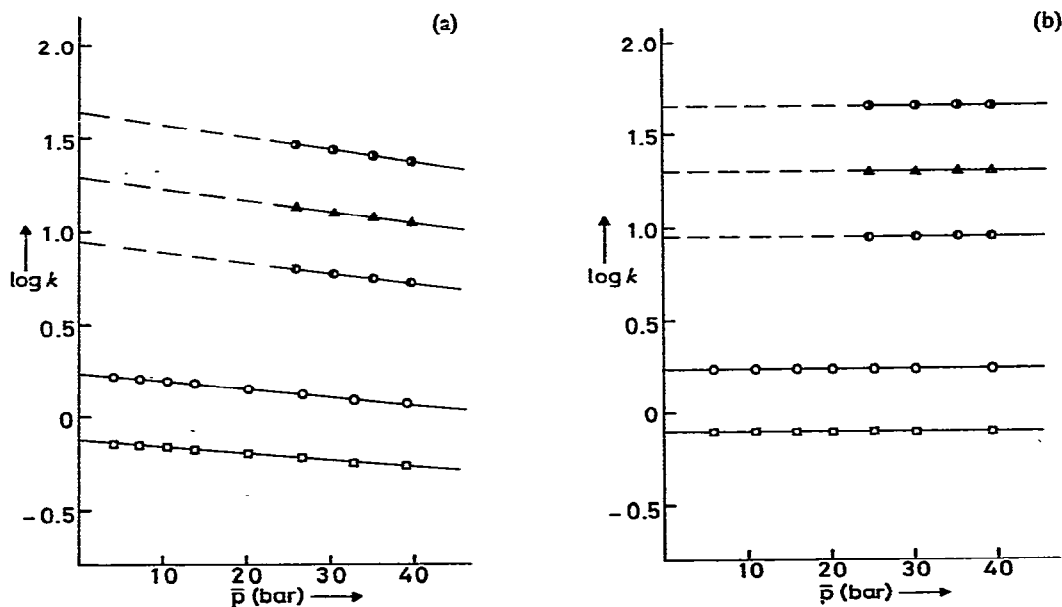


Fig. 14. Plot of $\log \kappa$ versus average column pressure (\bar{p}) for *n*-alkanes. Column, 1.0 mm I.D., length 6 m; packing, Spherosil XOC-005, 50–60 μm , coated with 3.0% (w/w) squalane; outlet pressure, atmospheric. Carrier gas: (a) nitrogen; (b) helium. Temperature, 80.0°. Other conditions as in Fig. 1. \square , *n*-pentane; \circ , *n*-hexane; \bullet , *n*-octane; \blacktriangle , *n*-nonane; \bullet , *n*-decane.

The influence of the pressure on the capacity ratio is distinct in nitrogen but insignificant in helium in the pressure range studied.

In agreement with theory^{13,14}, the dependence of the capacity ratio on pressure was found to be linear. It is possible to calculate activity coefficients and second cross-virial coefficients from plots as shown in Fig. 14. The second cross-virial coefficient describes the interaction between unlike molecules in the gas phase, *e.g.*, between solute and carrier gas. A more detailed investigation of this aspect will be described in a forthcoming paper.

Precision of sampling

With regard to analytical applications of the examples of separations shown in Figs. 8–10, the precision of the method was investigated. For each experiment the sample container (3 ml) was loaded with about 100 μ l of methane and 0.4 μ l of liquid per component; the static split was 1:150 in all instances, which means that about 1.5 μ g of each component was injected on to the column. The conditions were the same as in Figs. 8–10. The results are presented in Table VI.

TABLE VI
PRECISION OF SAMPLING ON 1.5-m AND 6-m COLUMNS

Type of compound	Compound*	1.5-m column			6-m column		
		\bar{X}^{**}	$S_{\bar{X}}$	$S_{\bar{X}}/\bar{X}$ (%)	\bar{X}^{**}	$S_{\bar{X}}$	$S_{\bar{X}}/\bar{X}$ (%)
Esters (conditions as in Fig. 8)	1	5.8	0.15	2.6	5.3	0.10	1.9
	2	7.3	0.26	3.6	6.9	0.32	4.7
	3	13.1	0.20	1.5	13.5	0.20	1.5
	4	17.3	0.12	0.7	17.3	0.30	1.7
	5	18.5	0.10	0.5	18.5	0.35	1.9
	6	17.4	0.20	1.1	17.1	0.25	1.5
	7	19.0	0.51	2.6	19.5	0.35	1.8
	8 (impurity)	1.3	0.15	11.3		(<i>n</i> =3)	
		(n=3)					
Light aromatic hydrocarbons (conditions as in Fig. 9)	1	3.9	0.17	4.4	3.9	0.06	1.5
	2	20.3	0.83	4.1	19.8	0.74	3.7
	3	15.6	0.76	4.9	15.9	0.56	3.5
	4	} 39.7	2.87	7.2	14.0	0.10	0.7
	5				13.3	0.17	1.3
	6				13.0	0.17	1.3
	7	12.4	0.90	7.3	11.8	0.40	3.4
	8	8.0	0.55	6.9	7.9	1.0	12.6
		(n=3)				(n=3)	
Lower alcohols (conditions as in Fig. 10)	1	6.0	0.34	5.7	7.6	0.29	3.8
	2	4.1	0.25	6.1	} 27.9	0.29	1.0
	3	26.2	0.52	2.0			
	4	} 23.6	0.57	2.4	13.3	0.20	1.5
	5				12.4	0.40	3.2
	6	13.0	0.13	1.0	11.9	0.10	0.8
	7	15.6	0.52	3.4	15.3	0.60	3.9
	8	11.7	1.35	11.6	11.1	0.40	3.6
		(n=4)				(n=3)	

* For identification of compounds, see legends to Figs. 8–10.

** \bar{X} = mean relative area.

From Table VI, it is obvious that for esters and light aromatic hydrocarbons the mean relative areas are approximately equal. With the lower alcohols the mean relative areas (\bar{X}) differ, probably owing to a lower resolution and a poorer peak shape or to adsorption outside the column. In all instances the precision is good, however, with the exception of some higher boiling components. The detrimental effects on precision can perhaps be diminished by a separate heating of the sample container and valve, and this aspect will be described in a forthcoming paper.

CONCLUSIONS

- (1) With a high pressure ratio, the number of theoretical plates increases proportionally with the column length.
- (2) A high pressure reduces the theoretical plate height and shifts its minimum value to lower flow velocities.
- (3) A small particle size significantly reduces the increase in theoretical plate height with flow velocity.
- (4) Pressure can change the retention sequence to some extent, depending on the carrier gas.
- (5) Packed columns comparable in efficiency to capillary columns can be prepared.

ACKNOWLEDGEMENTS

The authors thank Mr. E. C. Scheijde for this practical assistance in preparing the columns, Mr. K. Camstra for his technical advice and construction of the main parts of the apparatus and Packard-Becker N.V. (Delft, The Netherlands) for the gift of a prototype thermostat with a control unit of their 419 Series gas chromatographs.

REFERENCES

- 1 R. P. W. Scott, in D. H. Desty (Editor), *Gas Chromatography 1958*, Butterworths, London, 1958, p. 189.
- 2 M. N. Myers and J. C. Giddings, *Separ. Sci.*, 1 (1966) 761.
- 3 M. N. Myers and J. C. Giddings, *Anal. Chem.*, 37 (1965) 1453.
- 4 C. A. Cramers, J. Rijks and P. Boček, *J. Chromatogr.*, 65 (1972) 29.
- 5 C. A. Cramers, J. A. Rijks and P. Boček, *Clin. Chim. Acta*, 34 (1971) 159.
- 6 J. F. K. Huber, H. H. Lauer and H. Poppe, *J. Chromatogr.*, 112 (1975) 377.
- 7 J. F. K. Huber and J. A. R. J. Hulsman, *Anal. Chim. Acta*, 38 (1967) 305.
- 8 J. F. K. Huber, *J. Chromatogr. Sci.*, 7 (1969) 85.
- 9 J. F. K. Huber, in E. Kováts (Editor), *Column Chromatography*, *Chimia Suppl.*, Sauerländer, Aarau, 1970, p. 24.
- 10 J. F. K. Huber, *Ber. Bunsenges. Phys. Chem.*, 77 (1973) 159.
- 11 J. H. Knox and M. Saleem, *J. Chromatogr. Sci.*, 7 (1969) 614.
- 12 J. A. Rijks, *Characterization of Hydrocarbons by Gas Chromatography; Means of Improving Accuracy*, Thesis, Technical University of Eindhoven, The Netherlands, 1973.
- 13 D. H. Desty, A. Goldup, G. R. Luckhurst and W. T. Swanton, in M. van Swaay (Editor), *Gas Chromatography 1962*, Butterworths, London, 1962, p. 67.
- 14 S. T. Sie, W. van Beersum and G. W. A. Rijnders, *Separ. Sci.*, 1 (1966) 459.